Empirical tests of the black hole no-hair conjecture using gravitational-wave observations

Carullo, Gregorio; van der Schaaf, Laura; London, Lionel; Pang, Peter T. H.; Tsang, Ka Wa; Hannuksela, Otto A.; Meidam, Jeroen; Agathos, Michalis; Samajdar, Anuradha; Ghosh, Archisman

Published in:
Physical Review D

DOI:
10.1103/PhysRevD.98.104020

Publication date:
2018

Empirical tests of the black hole no-hair conjecture using gravitational -wave observations

Gregorio Carullo,[1,2,*] Laura van der Schaaf,[2] Lionel London,[3] Peter T. H. Pang,[4] Ka Wa Tsang,[2] Otto A. Hannuksela,[4] Jeroen Meidam,[2] Michalis Agathos,[5] Anuradha Samajdar,[2] Archisman Ghosh,[2] Tjonnie G. F. Li,[4] Walter Del Pozzo,[1,6] and Chris Van Den Broeck[2,7]

[1]*Dipartimento di Fisica "Enrico Fermi," Università di Pisa, Pisa I-56127, Italy*
[2]*Nikhef-National Institute for Subatomic Physics, Science Park, 1098 XG Amsterdam, Netherlands*
[3]*School of Physics and Astronomy, Cardiff University, The Parade, Cardiff CF24 3AA, United Kingdom*
[4]*Department of Physics, The Chinese University of Hong Kong, Shatin, NT, Hong Kong*
[5]*DAMTP, Centre for Mathematical Sciences, University of Cambridge, Wilberforce Road, Cambridge CB3 0WA, United Kingdom*
[6]*INFN sezione di Pisa, Pisa I-56127, Italy*
[7]*Van Swinderen Institute for Particle Physics and Gravity, University of Groningen, Nijenborgh 4, 9747 AG Groningen, Netherlands*

(Received 12 May 2018; published 15 November 2018)

We show that second-generation gravitational-wave detectors at their design sensitivity will allow us to directly probe the ringdown phase of binary black hole coalescences. This opens the possibility to test the so-called black hole no-hair conjecture in a statistically rigorous way. Using state-of-the-art numerical relativity-tuned waveform models and dedicated methods to effectively isolate the quasistationary perturbative regime where a ringdown description is valid, we demonstrate the capability of measuring the physical parameters of the remnant black hole and subsequently determining parameterized deviations from the ringdown of Kerr black holes. By combining information from $\mathcal{O}(5)$ binary black hole mergers with realistic signal-to-noise ratios achievable with the current generation of detectors, the validity of the no-hair conjecture can be verified with an accuracy of $\sim$1.5% at 90% confidence.

DOI: 10.1103/PhysRevD.98.104020

I. INTRODUCTION

The detection of gravitational waves (GWs) by the LIGO and Virgo Collaborations [1,2] has opened up a variety of avenues for the observational exploration of the dynamics of gravity and of the nature of black holes. GW150914 [3] and subsequent detections [4–9] have enabled unique tests of general relativity (GR) [5,6,8,10]. Among the several detections, GW150914 still holds a special place, not only because it was the first and the loudest binary black hole event detected, but also because it was the kind of textbook signal that allowed measurements of the frequency and damping time of what has been interpreted as the least damped quasinormal mode (QNM) of the presumed remnant black hole (BH) resulting from a binary black hole merger [10]. This sparked considerable interest in the community, since it opened up the prospect of more in-depth empirical studies of quasistationary Kerr black holes [11,12] in the near future, as the sensitivity of the Advanced LIGO and Advanced Virgo detectors is progressively improved [1,13]. Consistency with the prediction of GR hinted that the end result of GW150914 was indeed a Kerr black hole [14], but inability to detect more than one QNM did not yet allow tests of some key GR predictions for these objects. As first predicted by Vishveshwara [15] and further investigated by Press [16], and Chandrasekhar and Detweiler [17], in the regime where linearized general relativity is valid, the strain of the emitted gravitational-wave signal, at large distances from the BH and neglecting subdominant power-law tail contributions, takes the form

$$h(t) = \sum_{lmn} \mathcal{A}_{lmn} e^{-t/\tau_{lmn}} \cos(\omega_{lmn} t + \phi_{lmn}). \qquad (1)$$

For black holes in GR, all frequencies ω_{lmn} and damping times τ_{lmn} are completely determined by the black hole's mass and spin.[1] This can be viewed as a manifestation of the black hole no-hair conjecture, which essentially states that in GR, a stationary axisymmetric black hole is determined uniquely by its mass, intrinsic angular

*gregorio.carullo@ligo.org

[1]BH perturbation theory alone cannot predict the amplitudes $\mathcal{A}_{lmn}$ and relative phases ϕ_{lmn}; in the case of black holes resulting from a binary merger, these are set by the properties of the parent binary black hole system; see e.g., [18].

momentum, and electric charge (with the latter expected to be zero for astrophysical objects) [19–26]; see [27] for a review. This connection is key to several tests that have been proposed in the literature [28–36]. So far the possibility to verify (or refute) experimentally the no-hair conjecture has been explored mostly in the context of third-generation ground-based [37,38] or space-based [39] gravitational-wave detectors. In this work, we show that the existing advanced interferometric detector network, when operating at design sensitivity, will be capable of testing the no-hair conjecture with an accuracy of a few percent with the observation of the ringdown signal already for $\mathcal{O}(5)$ GW events.

All the mass quantities quoted in the remainder of the paper are defined in the reference frame of the detector. These are related to the masses in the source rest frame by a factor of $(1+z)$, with z the source redshift [40].

II. RINGDOWN MODEL

Our ringdown waveform model is that of Ref. [18], where a robust method was developed to characterize QNMs up to $l=5$, including overtones (labeled by the n index), by making use of numerical relativity (NR) waveforms. The Weyl scalar ψ_4 can be expanded as

$$\psi_4(\iota,\varphi,r,t) \simeq \frac{M}{r}\sum_{l,m,n}\psi_{lmn}(t)[{}_{-2}S_{lm}(a_f\tilde{\omega}_{lmn},\iota,\varphi)], \quad (2)$$

with

$$\psi_{lmn}(t) \equiv A_{lmn}e^{i\tilde{\omega}_{lmn}t}. \quad (3)$$

In the above, r is the distance from source to detector, (ι,φ) give the orientation of the ringing black hole with respect to the line of sight and ${}_{-2}S_{lm}$ are spin-weighted spheroidal harmonics. For the dependence of the complex mode frequencies $\tilde{\omega}\equiv\omega_{lmn}+i/\tau_{lmn}$ on the mass M_f and dimensionless spin a_f of the final black hole one can use the expressions from [31]. The *amplitudes* A_{lmn} of the various modes are set by the properties of the initial black holes that gave rise to the remnant object. As shown in [18], in the case of nonspinning progenitor objects, these are well captured by series expansions in the symmetric mass ratio $\eta\equiv m_1m_2/(m_1+m_2)^2$, with m_1 and m_2 the individual masses. The coefficients in these expansions are obtained by fitting against NR waveforms starting from a time $t=10M$ after the peak luminosity of the (2,2) component of $\psi_4^{\rm NR}$, with $M=m_1+m_2$; for details of the fitting procedure we refer to [18]. In this setup, the A_{lmn} are complex, so that they include relative phases between the modes, which were neglected in previous models [41] and subsequent Bayesian analyses that were based on them [29,32]; their inclusion leads to a significant improvement in faithfulness against NR waveforms [42]. At large distances from the source, the gravitational-wave polarizations h_+ and $h_\times$ are obtained from Eq. (2) through $\psi_4\simeq\ddot{h}_+-i\ddot{h}_\times$. The waveform model has recently been extended to the case of initial black holes with nonzero but aligned spins [42]. In this work we want to provide a proof of principle that linearized general relativity around a Kerr background can be directly probed with gravitational-wave observations with the current interferometric network, and the nonspinning model of [18] suffices to demonstrate this.

III. SIMULATIONS

Both to establish the effective ringdown start time and in subsequent simulations of no-hair conjecture tests, Bayesian parameter estimation is performed. The simulated signals are numerical inspiral-merger-ringdown waveforms taken from the publicly available Simulating eXtreme Spacetimes (SXS) catalog [43,44], with mass ratio $q=m_1/m_2$ in the interval [1,3] and negligible initial spins as well as negligible residual eccentricity (SXS:BBH:0001, SXS:BBH:0030, SXS:BBH:0169, SXS:BBH:0198). These are coherently injected into synthetic, stationary, Gaussian noise for a network of Advanced LIGO and Advanced Virgo detectors at design sensitivity [1,13]. The injected total mass is uniformly distributed in the interval $[50,90]\ M_\odot$, and the sky position as well as the orientation of the orbital plane at some reference time are uniformly distributed on the sphere. Luminosity distances D_L are chosen such that the total signal-to-noise ratio (SNR) in the inspiral-merger-ringdown signal approximately equals 100, which is a plausible value for signals similar to GW150914 [3] assuming the Advanced LIGO-Virgo network at full sensitivity. This sets the average SNR contained just in the ringdown phase of our data set to 15, if the start time is chosen to be $16M$ after the time at which the GW strain peaks (as will be demonstrated below, this is indeed a reasonable choice). By comparison, with the same choice of start time, the SNR in the ringdown of GW150914 with detectors at design sensitivity would have been $\mathrm{SNR}_{\rm ring}\simeq 17$ [10].

The template waveforms used in our Bayesian analyses follow the aforementioned ringdown model, augmented with a windowing procedure for the start time, as explained below. Sampling is done over ten parameters:

$$\{M_f,a_f,q,\alpha,\delta,\iota,\psi,D_L,t_c,\varphi_c\}, \quad (4)$$

where (α,δ) determine the sky location, ψ is the polarization angle and t_c and φ_c, respectively, are a reference time and phase. Hence only parameters associated with the ringdown waveform are sampled over, with the mass ratio q determining the mode amplitudes. Bayesian inference is done using the LALInference library [45]. Priors are chosen to be uniform in $[5,200]\ M_\odot$ for M_f, uniform in $[-1,1]$ for a_f, and uniform in $[1,15]$ for q. A constant

number density in comoving volume sets the prior for the sky location angles and the distance, with a distance range of [1, 1000] Mpc. The priors on (ι, ψ) are chosen to be uniform on the 2-sphere (with these angles being generated from the same distribution also for the simulation set). (For the SNRs considered, the impact of the specific shapes of the prior distributions has little impact on our results.) The time of coalescence is uniformly distributed within $[t_c - 0.1\ \mathrm{s}, t_c + 0.1\ \mathrm{s}]$, where t_c is a reference time at which the signal is detected.

IV. WHEN DOES THE RINGDOWN START?

The time at which the transition between the nonlinear to the linear regime happens is not well defined. For instance, Ref. [10] shows how the inference on the QNM central frequency and characteristic time changes quite dramatically depending on the assumed time at which the transition occurs. Therefore it is critical to make a reasonable choice for the time at which the remnant black hole can be treated perturbatively and assess the effectiveness of such a choice.

We choose the start time for the ringdown $t_{\rm start}$ from the analysis of numerical inspiral-merger-ringdown waveforms added to stationary Gaussian noise with a power spectral density as expected for Advanced LIGO and Virgo at design sensitivity [46]. To isolate the ringdown, we apply to the data a Planck [47] window whose starting time is varied in discrete steps over a range $[10, 20]M$ after the peak time of the strain in each detector, with M the total mass for the simulated signal.[2] The peak time $t_{\rm peak}$ itself can be estimated using analysis methods that can measure amplitudes and arrival times of a signal inside a detector, without relying on specific GR waveform models, such as BayesWave [48]. We choose a rise time for the Planck window of 1 ms, as we find that this choice gives a good compromise between the need to preserve the signal-to-noise-ratio and to avoid Gibbs phenomena. Consider a simulated signal with total mass M and mass ratio q, and a choice of window start time, e.g., $t_{\rm start} = t_{\rm peak} + \kappa M$ for some $\kappa \in [10, 20]$. We then apply a similar window on the ringdown template waveforms, letting them start at $\kappa M'$ after the peak strain, where the mass M' is obtained from the *sampled values* M'_f and q' through fitting formulas [49]. This leads to posterior density functions for all parameters and, in particular, for M_f and a_f. Our criterion to select the start time for the ringdown is built by minimizing the bias in the recovered parameters of the final object, while avoiding to select an arbitrarily large start time. Although large start times would ensure the validity of the linearized approximation employed in the waveform template, they would also drastically reduce the signal SNR, thus resulting in a poor estimation of the final parameters. The equilibrium point in this trade-off, arrived at as explained below, will ensure the analysis to take place in the linearized regime where our model is valid while still allowing a precise estimation of the measured parameters. By looking at the covariance between M_f and a_f and at the distance (induced by the covariance metric) between the true values M_f^I and a_f^I and the mean values $\bar{M}_f^I(\kappa)$ and $\bar{a}_f^I(\kappa)$, for each simulated signal I, we define the functions:

$$\mathcal{B}(\kappa, I) \equiv \sqrt{D_I^2(\kappa) + \det \mathbf{C}(\kappa)_I}, \tag{5}$$

$$D_I^2(\kappa) \equiv {}^t\Delta\vec{x}(\kappa)_I \mathbf{C}^{-1}(\kappa)_I \Delta\vec{x}(\kappa)_I, \tag{6}$$

where $\mathbf{C}(\kappa)_I$ is the two-dimensional covariance matrix between the posterior samples for M_f and a_f, $D_I(\kappa)$ is the (covariance induced) distance between the mean and the injected values and we defined the vector ${}^t\Delta\vec{x}(\kappa)_I = ((\bar{M}_f^I(\kappa) - M_f^I)/M_\odot, \bar{a}_f^I(\kappa) - a_f^I)$. The statistical uncertainty (larger for large start times), quantified by $\det \mathbf{C}(\kappa)_I$, is controlled by the signal-to-noise left in the ringdown part of the signal when the preceding stages are cut from the analysis. The distance $D_I(\kappa)$ quantifies the systematic uncertainty in the recovered parameters and is a proxy for the mismatch between the linear ringdown model and the nonlinear signal. We thus let the effective ringdown start time be the one that minimizes $\mathcal{B}(\kappa)$ (thus minimizing the combination of statistical and systematic uncertainties), defined as the average of $\mathcal{B}(\kappa, I)$ over all simulated signals. The data set consisted of 12 simulations at 11 different, equally spaced, values of $\kappa \in [10, 20]$, thus employing a total of 132 simulations. Figure 1 illustrates the procedure by showing 90% credible regions for M_f and a_f, together with the value of the *averaged* $\mathcal{B}(\kappa)$ as a function of the ringdown start time, for a particular system which had initial total mass $M = 72\ M_\odot$ and mass ratio $q = 1$. The value of κ minimizing $\mathcal{B}(\kappa)$ is $\kappa = 16$, which implies an effective ringdown start time of $t_{\rm start} = t_{\rm peak} + 16M$ after the peak strain of the signal. This is consistent with the conclusions stated in a independent study by Bhagwat *et al.*, using a "Kerrness" measure on a single GW150914-like numerical signal [11]. The selection of the ringdown start time at $t_{\rm start} = t_{\rm peak} + 16M$ uniquely determines the placement of the time-domain Planck window. When dealing with real signals, the window is initially applied once to the data with $t_{\rm start} = t_{\rm peak} + 16M_{\rm IMR}$, with $t_{\rm peak}$ from a model-independent reconstruction as explained above and $M_{\rm IMR}$ from a routine estimate (before performing our ringdown-only analysis) using an inspiral-merger-ringdown model.[3] While the posterior distribution for M

[2]The choice of a specific windowing function has no significant impact on the analysis as long as the frequency range of interest is not altered. We indeed verified that different tapering functions give nearly identical results.

[3]By studying a set of numerical simulations, we verified that different definitions of the fixed start time of the data window have a negligible impact on our results, since this choice just sets the amount of SNR being excluded from the analysis.

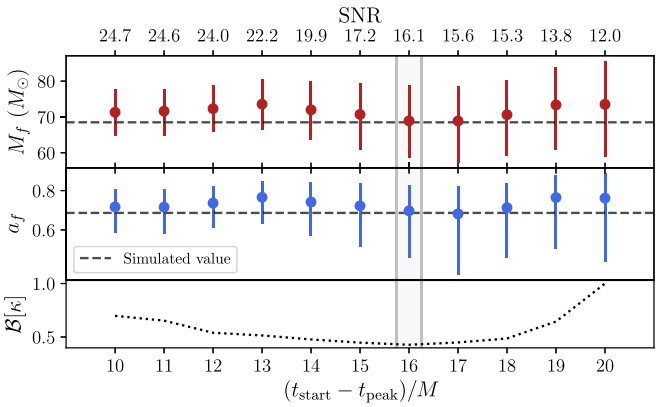

FIG. 1. Estimated median values and 90% credible regions for final mass M_f (top panel) and spin a_f (central panel) as a function of the start time of the ringdown with respect to the strain peak time $t_{\rm peak}$ for a simulation with $M_f = 68.5\ M_\odot$ and $a_f = 0.686$ (corresponding to $q = 1$). The bottom panel reports the value of the function $\mathcal{B}(k)$, averaged over *all* simulations. The gray box highlights the value of $t_{\rm start} - t_{\rm peak} = 16M$ for which $\mathcal{B}(k)$ is at a minimum.

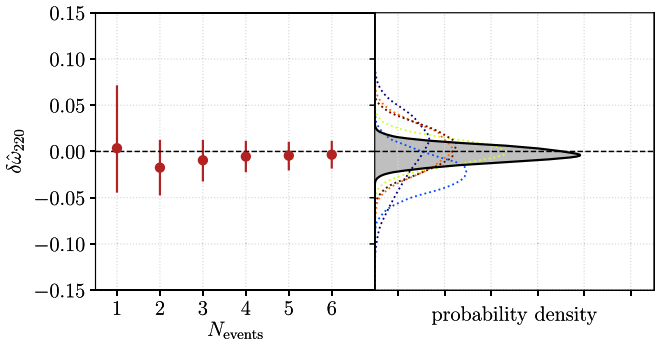

FIG. 2. Measurement of the departure of $\delta\hat{\omega}_{220}$ characterizing a departure of the dominant QNM frequency from its GR value, on a set of numerical simulations as described in the text. Left panel: Evolution of medians and 90% credible intervals from the joint posterior distribution. Right panel: Posterior probability densities for each individual signal (dotted lines) and the joint posterior distribution (solid line). With six detections the upper bound on $\delta\hat{\omega}_{220}$ is smaller than ∼1.5% at 90% confidence.

(obtained from the *sampled* values of M_f and q through fitting formulas) is being explored, the window on the template model is instead recalculated and reapplied at each step, with its starting time set to the proposed value $16M$ after the peak strain.

V. TESTING THE NO-HAIR CONJECTURE

As introduced in Refs. [29,32] in the context of third-generation detectors, we look for violations of the black hole no-hair conjecture by introducing linear deviations in the QNM parameters. In particular, we perturb around the QNM frequencies and damping times as predicted by GR as

$$\begin{aligned}\omega_{lmn}(M_f, a_f) &\to (1 + \delta\hat{\omega}_{lmn})\omega_{lmn}(M_f, a_f),\\ \tau_{lmn}(M_f, a_f) &\to (1 + \delta\hat{\tau}_{lmn})\tau_{lmn}(M_f, a_f),\end{aligned} \tag{7}$$

where $\delta\hat{\omega}_{lmn}$ and $\delta\hat{\tau}_{lmn}$ are relative deviations that we include as additional degrees of freedom in our inference. The parameterization in (7) has the advantages of being agnostic to specific families of violations and, most importantly, to be uniquely defined in GR, $\delta\hat{\omega}_{lmn} = \delta\hat{\tau}_{lmn} \equiv 0\ \forall\ l, m, n$. The no-hair conjecture constrains the number of independent degrees of freedom of an axisymmetric black hole in GR to be two; therefore, the conjecture is tested by measuring at least three independent parameters characterizing the remnant geometry, which we chose to be M_f, a_f, and $\delta\hat{\omega}_{220}$. In addition, the algorithm also samples all the other parameters as specified above. The priors are unchanged except on M_f and a_f, where we restrict to values contained in the 90% credible intervals obtained from an earlier analysis including inspiral and merger. The prior on $\delta\hat{\omega}_{220}$ is chosen to be uniform in $[-1, 1]$. We consider GR signals with mass ratio $q \leq 3$, for which the best QNM determined parameter is the frequency for the least-damped (2,2,0) mode. We thus focus on the accuracy of the measurement of $\delta\hat{\omega}_{220}$. Figure 2 shows the results of an analysis performed on a set of inspiral-merger-ringdown signals added to stationary Gaussian noise as described above. Upper bounds on the departures from the predictions of GR for ω_{220} are smaller than ∼1.5% at the 90% credible level already with six sources, while upper bounds on deviations from τ_{220} predictions are smaller than $\mathcal{O}(10\%)$. On the selected data set higher modes deviations on both frequency and damping time are essentially unconstrained.

VI. CONCLUSIONS

In this work, we demonstrated that observationally testing the black hole no-hair conjecture is possible within the next few years, once the LIGO-Virgo detector network reaches its design sensitivity. The ability to isolate the quasilinear ringdown regime from the nonlinear merger stage of the coalescence process enables estimating the parameters characterizing the ringdown. This also allows the identification of the time of the transition to be $16M$ after the peak strain, M being the total mass of the merging system. Following our procedure, we showed that, with just $\mathcal{O}(5)$ plausible signals, violations from the no-hair conjecture, seen as changes in the dominant QNM frequency and damping time, can be constrained to be smaller than, respectively, ∼1.5% and ∼10% at 90% confidence. The results presented in this work can be extended to the recent spin-aligned ringdown model from Ref. [42]. This and results for actual signals in LIGO and Virgo data are deferred to a later publication.

ACKNOWLEDGMENTS

G. C. would like to thank Alessandro Nagar for helpful discussions. The authors would like to thank Maria Haney for a critical reading of the manuscript and for valuable suggestions towards its improvement. L. v. d. S., K. W. T., J. M., A. S., A. G., and C. V. D. B. are supported by the research program of the Netherlands Organisation for Scientific Research (NWO). P. T. H. P., O. A. H., and T. G. F. L. are partially supported by a grant from the Research Grants Council of the Hong Kong (Project No. CUHK 24304317) and the Direct Grant for Research from the Research Committee of the Chinese University of Hong Kong. O. A. H. is also supported by the Hong Kong Ph.D. Fellowship Scheme (HKPFS) issued by the Research Grants Council (RGC) of Hong Kong. M. A. acknowledges NWO-Rubicon Grant No. RG86688. W. D. P. is funded by the "Rientro dei Cervelli Rita Levi Montalcini" Grant of the Italian MIUR. We are grateful for computational resources provided by Cardiff University and funded by an STFC grant supporting UK Involvement in the Operation of Advanced LIGO. This work greatly benefited from discussions within the *strong-field* working group of the LIGO/Virgo Collaboration.

Note added.—While this work was being finalized, a study by Brito and collaborators [36] appeared as a preprint. Although the method proposed is substantially different, their conclusions are similar to ours.

[1] F. Acernese *et al.* (Virgo Collaboration), Classical Quantum Gravity **32**, 024001 (2015).
[2] B. P. Abbott *et al.*, Living Rev. Relativity **21**, 3 (2018).
[3] B. P. Abbott *et al.* (LIGO Scientific and Virgo Collaborations), Phys. Rev. Lett. **116**, 061102 (2016).
[4] B. P. Abbott *et al.* (LIGO Scientific and Virgo Collaborations), Phys. Rev. Lett. **116**, 241103 (2016).
[5] B. P. Abbott *et al.* (Virgo and LIGO Scientific Collaborations), Phys. Rev. X **6**, 041015 (2016).
[6] B. P. Abbott *et al.* (Virgo and LIGO Scientific Collaborations), Phys. Rev. Lett. **118**, 221101 (2017).
[7] B. P. Abbott *et al.* (Virgo and LIGO Scientific Collaborations), Astrophys. J. **851**, L35 (2017).
[8] B. P. Abbott *et al.* (LIGO Scientific and Virgo Collaborations), Phys. Rev. Lett. **119**, 141101 (2017).
[9] B. P. Abbott *et al.* (LIGO Scientific and Virgo Collaborations), Phys. Rev. Lett. **119**, 161101 (2017).
[10] B. P. Abbott *et al.* (LIGO Scientific and Virgo Collaborations), Phys. Rev. Lett. **116**, 221101 (2016).
[11] S. Bhagwat, M. Okounkova, S. W. Ballmer, D. A. Brown, M. Giesler, M. A. Scheel, and S. A. Teukolsky, Phys. Rev. D **97**, 104065 (2018).
[12] M. Cabero, C. D. Capano, O. Fischer-Birnholtz, B. Krishnan, A. B. Nielsen, and A. H. Nitz, Phys. Rev. D **97**, 124069 (2018).
[13] B. P. Abbott *et al.* (Virgo and LIGO Scientific Collaborations), Living Rev. Relativity **19**, 1 (2016); **21**, 3 (2018).
[14] R. P. Kerr, Phys. Rev. Lett. **11**, 237 (1963).
[15] C. V. Vishveshwara, Phys. Rev. D **1**, 2870 (1970).
[16] W. H. Press, Astrophys. J. **170**, L105 (1971).
[17] S. Chandrasekhar and S. L. Detweiler, Proc. R. Soc. A **344**, 441 (1975).
[18] L. London, D. Shoemaker, and J. Healy, Phys. Rev. D **90**, 124032 (2014).
[19] V. Ginzburg and L. Ozernoy, Zh. Eksp. Teor. Fiz. **147**, 1030 (1964).
[20] A. Doroshkevic, Y. B. Zeldovich, and I. Novikov, Sov. Phys. JETP **36**, 1 (1965).
[21] W. Israel, Phys. Rev. **164**, 1776 (1967).
[22] B. Carter, Phys. Rev. Lett. **26**, 331 (1971).
[23] S. W. Hawking, Commun. Math. Phys. **25**, 152 (1972).
[24] D. C. Robinson, Phys. Rev. Lett. **34**, 905 (1975).
[25] P. O. Mazur, J. Phys. A **15**, 3173 (1982).
[26] G. Bunting, Ph.D. thesis, University of New England, Armidale, N.S.W., 1983 (unpublished).
[27] P. O. Mazur, arXiv:hep-th/0101012.
[28] O. Dreyer, B. J. Kelly, B. Krishnan, L. S. Finn, D. Garrison, and R. Lopez-Aleman, Classical Quantum Gravity **21**, 787 (2004).
[29] S. Gossan, J. Veitch, and B. S. Sathyaprakash, Phys. Rev. D **85**, 124056 (2012).
[30] V. Ferrari and L. Gualtieri, Gen. Relativ. Gravit. **40**, 945 (2008).
[31] E. Berti, V. Cardoso, and C. M. Will, Phys. Rev. D **73**, 064030 (2006).
[32] J. Meidam, M. Agathos, C. Van Den Broeck, J. Veitch, and B. S. Sathyaprakash, Phys. Rev. D **90**, 064009 (2014).
[33] H. Yang, K. Yagi, J. Blackman, L. Lehner, V. Paschalidis, F. Pretorius, and N. Yunes, Phys. Rev. Lett. **118**, 161101 (2017).
[34] C. F. Da Silva Costa, S. Tiwari, S. Klimenko, and F. Salemi, Phys. Rev. D **98**, 024052 (2018).
[35] E. Thrane, P. D. Lasky, and Y. Levin, Phys. Rev. D **96**, 102004 (2017).
[36] R. Brito, A. Buonanno, and V. Raymond, Phys. Rev. D **98**, 084038 (2018).
[37] M. Punturo *et al.*, Classical Quantum Gravity **27**, 194002 (2010).
[38] B. P. Abbott *et al.* (LIGO Scientific Collaboration), Classical Quantum Gravity **34**, 044001 (2017).
[39] K. Danzmann, Classical Quantum Gravity **13**, A247 (1996).
[40] A. Krolak and B. F. Schutz, Gen. Relativ. Gravit. **19**, 1163 (1987).
[41] I. Kamaretsos, M. Hannam, S. Husa, and B. S. Sathyaprakash, Phys. Rev. D **85**, 024018 (2012).
[42] L. T. London, arXiv:1801.08208.

[43] A. Mroue *et al.*, Phys. Rev. Lett. **111**, 241104 (2013).
[44] J. Blackman, S. E. Field, C. R. Galley, B. Szilgyi, M. A. Scheel, M. Tiglio, and D. A. Hemberger, Phys. Rev. Lett. **115**, 121102 (2015).
[45] J. Veitch *et al.*, Phys. Rev. D **91**, 042003 (2015).
[46] Advanced LIGO anticipated sensitivity curves, LIGO Document No. T0900288-v3, https://dcc.ligo.org/LIGO-T0900288/public.
[47] D. J. A. McKechan, C. Robinson, and B. S. Sathyaprakash, Classical Quantum Gravity **27**, 084020 (2010).
[48] N. J. Cornish and T. B. Littenberg, Classical Quantum Gravity **32**, 135012 (2015).
[49] X. Jiménez-Forteza, D. Keitel, S. Husa, M. Hannam, S. Khan, and M. Pürrer, Phys. Rev. D **95**, 064024 (2017).